Annual Journal of Hydraulic Engineering, JSCE, Vol.54, 2010, February

FUNDAMENTAL STUDY OF BINGHAM FLUID BY MEANS OF DAM-BREAK FLOW MODEL

How Tion PUAY[1] and Takashi HOSODA[2]

[1] Member of JSCE, Phd Student, Dept. of Urban Management, Kyoto University (Kyodai Katsura, Nishikyo-ku, Kyoto 615-8530, Japan)

[2]Member of JSCE, Professor, Dept. of Urban Management, Kyoto University (Kyodai Katsura, Nishikyo-ku, Kyoto 615-8530, Japan)

This paper presents a fundamental study of Bingham fluid by means of dam-break flow model. A numerical model based on a two-dimensional free-surface VOF (Volume of Fluid) method is developed to simulate the slump flow test of fresh concrete and used to verify the characteristic flow phases of Bingham fluid. The advection terms in the Navier-Stokes equations are solved using CIP (Cubic-Interpolated Propagation) scheme. The advection of VOF density function, *F* is also solved with CIP scheme. The reliability of the numerical model is verified with available experimental results of slump flow test.

Key Words: *Bingham fluid, dam-break flow, CIP scheme, slump flow test*

1. INTRODUCTION

Dam-break flow model is a ubiquitous model used in the study of shallow flow. The author previously used dam-break flow of finite volume to study the characteristic flow phases for viscous Newtonian and non-Newtonian fluid by deriving similarity solution for the propagation of front position and the depth of flow at the origin[1)]. In the case of viscous fluid, characteristic flow phases exist[2)]. When the flow motion is governed by the inertial of the flow, it is said that the flow is in inertial flow phase. Consequently, when the viscosity of the fluid becomes more dominant, the flow enters a viscous flow phase where the motion is governed by the viscous– pressure equilibrium[1),2)].

Based on the dam-break flow of finite volume model, Kokado et al[3),4)] carried out studies on the rheological properties and flow characteristics of fresh concrete which was treated as a kind of Bingham fluid. In the works of Kokado et al[4)], a numerical model based on the Marker and Cell (MAC) method was used to simulate slump flow test, and the numerical results were compared with results from experimental works. However, in some cases it was reported that the numerical model could not produce satisfactory results especially in the case where the ratio of yield stress-plastic viscosity is less than 1.0[4)]. In this study, a numerical model based on the VOF method coupled with higher order scheme CIP, hereafter referred as VOF-CIP model will be used to reproduce the slump flow test and characteristic flow phases of Bingham fluid.

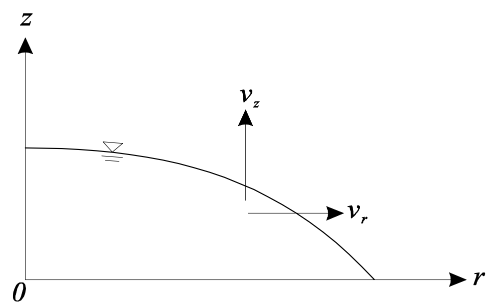

Fig.1 Dam-break flow of finite volume in cylindrical coordinate system used in this study.

2. GOVERNING EQUATIONS

The slump flow test problem can be regarded as an axis-symmetry flow problem. Therefore, the slump flow test problem can be reduced to a two-dimensional dam-break flow of finite volume shown in **Fig. 1** with its origin situated at the center of the slump flow. The motion slump flow in a two-dimensional model can be described by the following equation of motions,

Continuity equation:

$$\frac{1}{r}\frac{\partial}{\partial r}(rv_r)+\frac{\partial v_z}{\partial z}=0 \tag{1}$$

Momentum equation:

$$\begin{aligned}&\frac{\partial v_r}{\partial t}+\frac{1}{r}\frac{\partial(rv_r^2)}{\partial r}+\frac{\partial(v_r v_z)}{\partial z}\\&=-\frac{1}{\rho}\frac{\partial P}{\partial r}+\frac{\eta}{\rho}\left[\frac{\partial}{\partial r}\left(\frac{1}{r}\frac{\partial(rv_r)}{\partial r}\right)+\frac{\partial^2 v_r}{\partial z^2}\right]+g_r\end{aligned} \tag{2a}$$

$$\begin{aligned}&\frac{\partial v_z}{\partial t}+\frac{1}{r}\frac{\partial(rv_r v_z)}{\partial r}+\frac{\partial(v_z^2)}{\partial z}\\&=-\frac{1}{\rho}\frac{\partial P}{\partial z}+\frac{\eta}{\rho}\left[\frac{1}{r}\frac{\partial}{\partial r}\left(\frac{1}{r}\frac{\partial v_z}{\partial r}\right)+\frac{\partial^2 v_r}{\partial z^2}\right]+g_z\end{aligned} \tag{2b}$$

where v_r is the velocity in r-direction, v_z is the velocity in z-direction, r is the radius measured from the origin, ρ is the density of the fluid, η is the viscosity of the fluid, g_z and g_r are gravity acceleration components in z and r directions respectively and P is pressure.

3. NUMERICAL SIMULATION OF SLUMP FLOW TEST

The numerical model used to simulate the slump flow test of fresh concrete is based on the Volume of Fluid (VOF) method[5]. The governing equations for the numerical model are the continuity and momentum equations in cylindrical coordinate system as in Eq. (1), (2a) and (2b).

(1) Constitutive relations of Bingham fluid

The constitutive relations for Bingham fluid based on the extension by Hohenemser and Prager in arbitrary stress state[6] can be written as follows:

$$2\eta_{pl}e_{ij}=\begin{cases}0 & \text{for } \sqrt{J_2'}\le\tau_y\\ \left(1-\dfrac{\tau_y}{\sqrt{J_2'}}\right)\tau_{ij}' & \text{for } \sqrt{J_2'}>\tau_y\end{cases} \tag{3}$$

where τ_{ij}' is the stress-deviation tensor, η_{pl} is the plastic viscosity, e_{ij} is the strain rate tensor and τ_y is the yield stress. J_2' is the second invariant of stress-deviation tensor defined as follows,

$$\begin{aligned}J_2'=&\frac{1}{2}\left({\tau_{rr}'}^2+{\tau_{\theta\theta}'}^2+{\tau_{zz}'}^2\right)\\&+{\tau_{r\theta}'}^2+{\tau_{\theta z}'}^2+{\tau_{zr}'}^2\end{aligned} \tag{4}$$

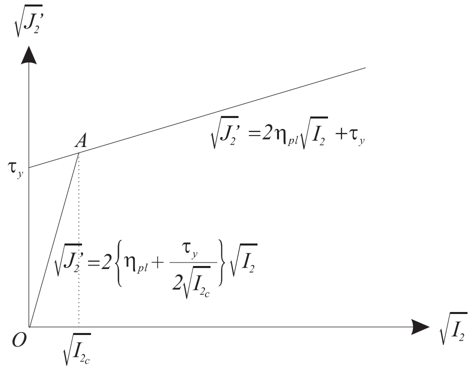

Fig.2 Bi-linear model used in the numerical model.

Based on the constitutive relation in Eq. (3), Kokado et al[4] proposed a bi-linear model for the numerical model where the following relation between stress - deviation tensor, τ'_{ij} and second invariant strain rate tensor I_2 in Eq (5) holds. This bi-linear model is adapted in the numerical model in this study.

$$\tau'_{ij}=\begin{cases}2\left(\eta_{pl}+\dfrac{\tau_y}{2\sqrt{I_2}}\right)e_{ij} & \text{for } \sqrt{J_2'}>\tau_y\\ 2\left(\eta_{pl}+\dfrac{\tau_y}{2\sqrt{I_{2_c}}}\right)e_{ij} & \text{for } \sqrt{J_2'}\le\tau_y\end{cases} \tag{5}$$

The second invariant strain rate tensor I_2 is ,

$$I_2=\frac{1}{2}\left(e_{rr}^2+e_{\theta\theta}^2+e_{zz}^2\right)+e_{r\theta}^2+e_{\theta z}^2+e_{z\theta}^2 \tag{6}$$

I_{2_c} is the critical value of second invariant strain rate tensor which is used to the determine the slope of line OA in **Fig. 2.** The value of $I_{2_c}=0.03s^{-1}$ is used in the numerical model based on the works of Kokado et al[4]. It can be seen from **Fig. 2** that the bilinear model is used because without introducing a second linear line OA, the value of $\sqrt{\mathrm{J}_2'}$ cannot be determined in the case where $\sqrt{\mathrm{J}_2'}<\tau_\mathrm{y}$ which causes problem in numerical simulation.

The total stress, σ_{ij} in the equation of motion is,

$$\begin{aligned}\sigma_{ij}&=-p\delta_{ij}+\tau'_{ij}\\&=-p\delta_{ij}+2\eta e_{ij}\end{aligned} \tag{7}$$

where δ_{ij} is the Kronecker delta. By comparing Eq. (7) with Eq.(5), we can expressed the viscosity η as follows,

$$\eta=\begin{cases}\eta_{pl}+\dfrac{\tau_y}{2\sqrt{I_2}} & \text{for } \sqrt{I_2}>\sqrt{I_{2_c}}\\ \eta_{pl}+\dfrac{\tau_y}{2\sqrt{I_{2c}}} & \text{for } \sqrt{I_2}\le\sqrt{I_{2_c}}\end{cases} \tag{8}$$

In the numerical model, the second invariant strain rate I_2 is calculated using Eq. (6) and used to determine the viscosity expressed in Eq. (8).

(2) Numerical model

The numerical simulation of slump flow test of fresh concrete is carried out using the Volume of Fluid (VOF) method by Hirt et al[5]. The advection terms in the momentum equations of Eq. (2a) and (2b) are solved using CIP scheme which is a less diffusive, higher order scheme. In the advection of VOF density function F, CIP scheme is used as well instead of the conventional donor-acceptor method.

a) CIP Scheme

A two-dimensional solver CIP scheme can be used to solve the advection equation of the following form[7],

$$\frac{\partial f}{\partial t}+u\frac{\partial f}{\partial x}+v\frac{\partial f}{\partial y}=0 \tag{9}$$

The advection terms in Eq. (2a) and (2b) can be solved using the two-dimensional solver of CIP scheme. However, the advection terms in Eq.(2a) and (2b) need to be re-arranged before CIP scheme can be used. Taking Eq. (2a) as an example, the conservative form of the advection term can be reduced to the form of Eq. (9) by using continuity equation in Eq. (1) as follows,

$$\begin{aligned}&\frac{\partial v_r}{\partial t}+\frac{1}{r}\frac{\partial (r v_r^2)}{\partial r}+\frac{\partial (v_r v_z)}{\partial z}\\&=\frac{\partial v_r}{\partial t}+v_r\frac{\partial v_r}{\partial r}+v_z\frac{\partial v_z}{\partial z}+v_r\left[\frac{1}{r}\frac{\partial (r v_r)}{\partial r}+\frac{\partial v_z}{\partial z}\right]\\&=\frac{\partial v_r}{\partial t}+v_r\frac{\partial v_r}{\partial r}+v_z\frac{\partial v_z}{\partial z}\end{aligned} \tag{10}$$

The same method applies to the advection term in Eq. (2b) where it can be reduced to the form of Eq. (9) by using continuity equation of Eq. (1). However, CIP method cannot be used directly to solve the advection equations in momentum equations of Eq. (2a) and (2b) because of the non-advection terms on the right hand side of the equations (the viscosity, pressure and gravity acceleration term). The method to solve the advection terms with CIP scheme in the presence of non-advection terms is explained in reference[7] where these equations are solved in two stages: the non-advection stage and advection stage.

The two-dimensional CIP solver is used to solve the advection of VOF density function F as well. Instead of the non-conservative form of F function used in the original VOF method[5], the following conservative form in cylindrical coordinate system is used,

$$\frac{\partial f}{\partial t}+\frac{1}{r}\frac{\partial (r v_r f)}{\partial r}+\frac{\partial (v_z f)}{\partial z}=0 \tag{11}$$

Eq. (11) is re-arranged to the form of Eq. (9) as follows,

$$\frac{\partial f}{\partial t}+v_r\frac{\partial f}{\partial r}+v_z\frac{\partial f}{\partial z}=-f\left(\frac{1}{r}\frac{\partial (r v_r)}{\partial r}+\frac{\partial v_z}{\partial y}\right) \tag{12}$$

The left hand side of Eq. (12) is the advection term and the right hand side is the non-advection term. Therefore, Eq. (12) can be solved using the method mentioned above for momentum equation, where it is solved in two stages: the non-advection stage and advection stage. In order to improve the performance of the advection of the VOF density function F, especially in maintaining sharp surface, a digitizer function[8] of the following form is used,

$$h=\tan\,[\,0.85\pi(F-0.5)] \tag{13}$$

Instead of directly using F value, h value is used in the CIP solver, and the new value of h after advection is inversed to obtain the new value of F as in the following equation,

$$F=\frac{1}{0.85\pi}tan^{-1}\,h+0.5 \tag{14}$$

(3) Simulation conditions

a) Numerical model setup

The cell size in the radial direction Δr and vertical direction Δz are set as 5mm in each direction. Time increment Δt is set as 1.0×10^{-5}s and adjusted for stability based on the following criteria[5],

$$\Delta t<min\left[\frac{\Delta r}{|v_{r_{ij}}|},\frac{\Delta z}{|v_{z_{ij}}|}\right] \tag{15}$$

$$\eta\Delta t<\frac{1}{2}\,\frac{\Delta r^2\,\Delta z^2}{\Delta r^2\,+\,\Delta\,z^2} \tag{16}$$

where $v_{r_{ij}}$ and $v_{z_{ij}}$ are velocity V_r and V_z in cell ij respectively.

b) Boundary conditions

The vertical axis at the origin is set as slip-condition representing the condition at the axis-symmetry axis in the actual slump flow test. The bottom floor is set as non-slip conditions. The slump cone wall effect is included in the simulation by setting non-slip condition along the cone wall. The pulling rate of the cone is 40mms^{-1} based on the experimental work by Kokado et al[4]. Non-slip condition is set for the cone wall.

c) Initial conditions and flow radius measurement

The initial shape of the fresh-concrete slump is shown in **Fig. 3**. A 5mm or 1 cell opening is present at the beginning of the numerical simulation. The position of the front of the slump, which is called the flow radius in this study, is measured in the numerical simulation.

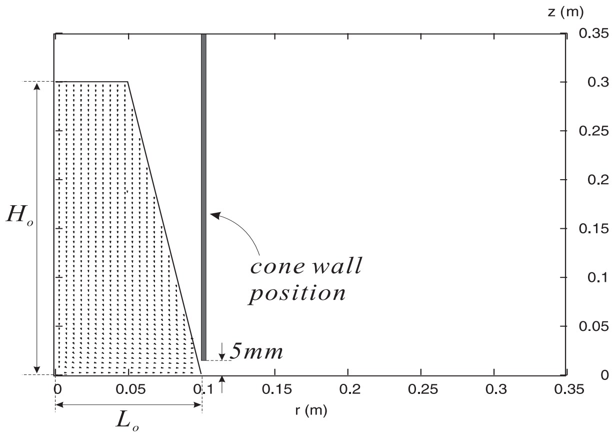

Fig.3 Initial condition of slump flow in numerical simulation.

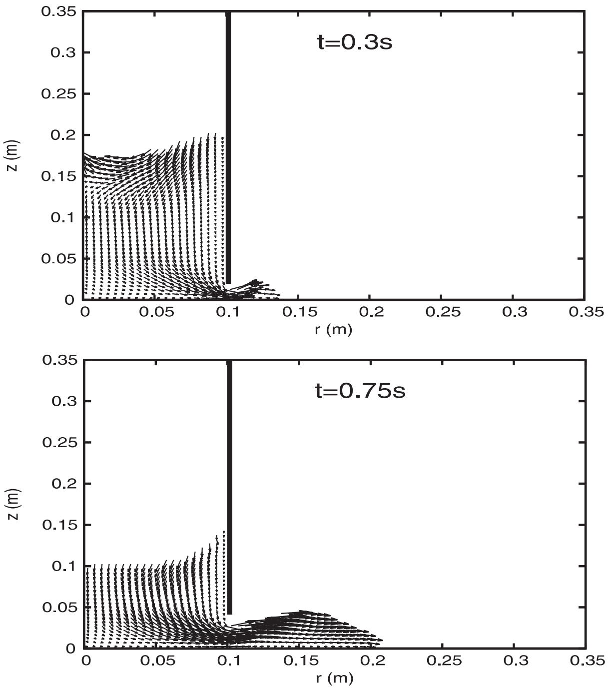

Fig.4 Simulation of slump flow test for case M35-7

As measurement of flow radius starts as soon as the cone is lifted in the experimental work, time is set to zero when the flow radius reaches 110mm in both numerical model and experimental work. This overcomes the discrepancy between the numerical model (due to the initial 5mm opening) and experimental works.

d) Rheological properties

In order to compare the numerical simulation results with the experimental work of slump flow test carried out by Kokada et al[4], similar rheological properties of fresh concrete are used. The rheological properties used in the numerical simulations are summarized in **Table 1.**

e) Results and performance of numerical model

The simulation of slump flow test for case M35-7 is shown in **Fig. 4**. The effect of the cone wall pulling can be seen where the fresh concrete near

Table 1 Rheological property for numerical simulation cases.

Exp no	ρ (kgm^{-3})	τ_y (Pa)	η_{pl} $(Pa.s)$
M025-1	2187	112	44
M025-2	2187	72	43
M30-1	2237	121	60
M30-4	2237	34	28
M30-7	2237	10	21
M35-1	2187	102	33
M35-2	2187	106	18
M35-4	2187	32	15
M35-6	2187	15	11
M35-7	2187	12	9.8
M40-3	2140	10	4.7
M050-4	2187	35	53
M050-6	2187	24	42
M050-7	2187	11	33

the wall is pulled up. The performance of the VOF-CIP model in this study is compared with the experimental and MAC model results carried out by Kokado et al[4] as shown in **Fig. 5a** to **Fig. 5c**. Three cases showing different degree of agreement between numerical models and experimental results are shown. It can be seen that the VOF-CIP model performed better than the MAC model in the case where the ratio of $\eta/\tau_y < 1.0$ as in **Fig. 5 a)**. This overcomes the problem reported by Kokado et al[4] that the MAC model performance was unsatisfactory for cases with $\eta/\tau_y < 1.0$. However, the MAC method performed better when the ratio $\eta/\tau_y > 1.0$ as in **Fig. 5 b)**. The VOF-CIP model matched the experimental result better compared to the MAC model as in **Fig. 5 c)**. Due to the lack of data from the MAC model, it is hard to conclude that one model is more reliable than the other one based on the comparison of three cases only. The VOF-CIP model is used to reproduce the characteristic flow phases of Bingham fluid in the following section.

4. CHARACTERTISTIC FLOW PHASES IN BINGHAM FLUID

In the study of Hosoda et al[9], the Bingham fluid characteristic flow phases are derived in terms of power-law solutions based on the assumption of self-similarity in the inertial and viscous flow phases by using the dam-break flow of finite volume model. The model of study was based on the following depth averaged model in cylindrical coordinate system,

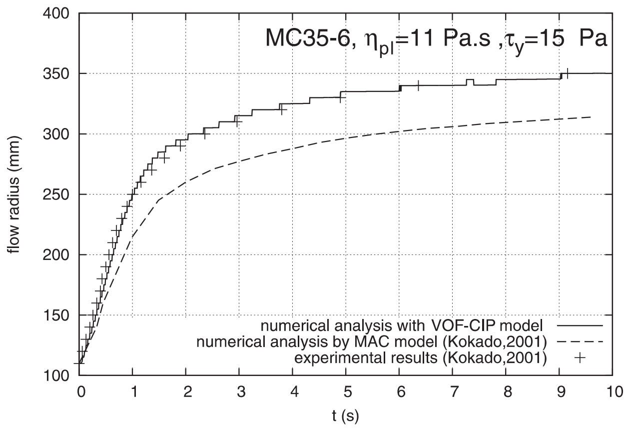

Fig. 5a Flow radius for case M35-6 for VOF-CIP and MAC model and experimental works by Kokado[4)]

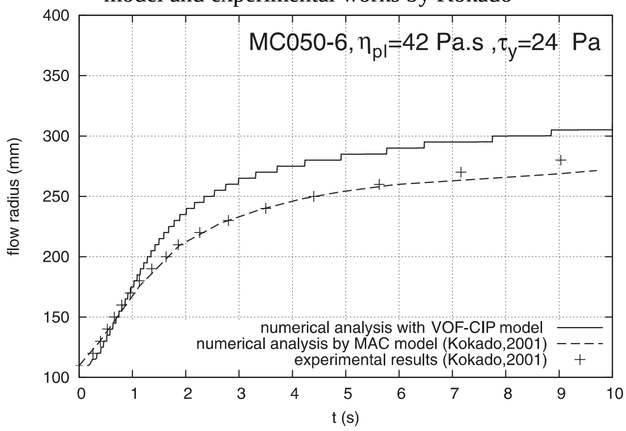

Fig. 5b Flow radius for case M050-6 for VOF-CIP and MAC model and experimental works by Kokado[4)]

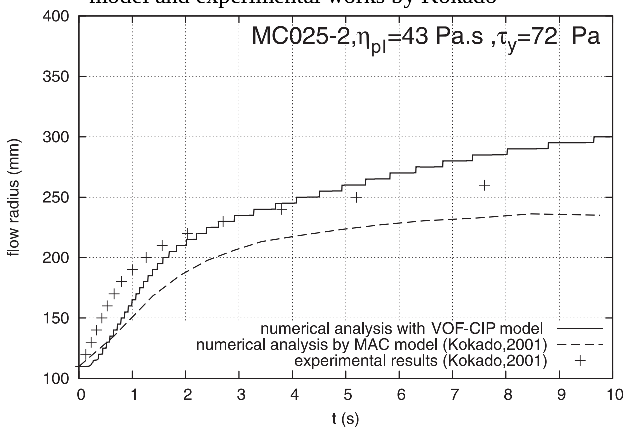

Fig. 5c Flow radius for case M025-2 for VOF-CIP and MAC model and experimental works by Kokado[4)]

$$\frac{\partial h}{\partial t} + \frac{1}{r}\frac{\partial (rh\partial U_r)}{\partial r} = 0 \tag{17}$$

$$\frac{\partial (hU_r)}{\partial t} + \frac{1}{r}\frac{\partial (r\beta h\partial U_r^2)}{\partial r} + gh\frac{\partial h}{\partial r} = -\frac{3U_r}{h}\frac{\eta}{\rho} \tag{18}$$

with h as the depth of flow, U_r as the depth averaged flow velocity in r direction, β as the momentum coefficient assumed as $\beta = 1$ and g as the gravity acceleration. Through the assumption of self similarity, the depth $h(r,t)$ and flow velocity $U_r(r,t)$ were expressed by the similarity functions $p(r/L)$ and $q(r/L)$ in the analysis as follows,

$$h = h_m(t)p\left(\frac{r}{L}\right) \tag{19}$$

$$U_r = U_m(t)q\left(\frac{r}{L}\right) \tag{20}$$

The function h_m and U_m and front position of the flow L were expressed as follows,

$$h_m = \alpha h_o\left(\sqrt{g/h_o}\,t\right)^a \tag{21}$$

$$U_m = \beta\sqrt{gh_o}\left(\sqrt{g/h_o}\,t\right)^b \tag{22}$$

$$L = \gamma L_o\left(\sqrt{g/h_o}\,t\right)^c \tag{23}$$

where $\alpha, \beta, \gamma, a, b, c$ are dimensionless coefficients, h_o and L_o are the initial depth and width of the dam respectively. The solutions of the coefficient a, b, c were found by equating pressure term with inertial term for inertial flow phase and pressure term with viscous term for viscous flow phase. The results relating to the propagation of flow front position L is used to verify the characteristic flow phases of numerical model in this study. The solution for coefficient c[9)] relating to the propagation of the flow front position is summarized as follows,

$$c = 1/2 \text{ for inertial phase flow} \tag{24}$$

$$c = 1/8 \text{ for viscous phase flow} \tag{25}$$

(1) Verification of characteristic flow phases

The flow radius propagation is plotted in three extreme cases where the yield stress is relatively low, mild and high in **Fig. 6 a), b)** and **c)** respectively. Low yield stress cases are MC050-7, MC30-7, MC35-7 and MC40-3. Mild yield stress cases are MC050-4, MC030-4 and MC35-4. High yield stress cases are MC30-1, MC025-1, MC35-1 and MC35-2. In each case, two distinct flow phases can be observed. In the inertial phase flow, the characteristic of inertial flow can be observed in case where the yield stress is relatively low and mild. In the case of relatively high yield stress, the inertial flow characteristic is not distinct. As the yield stress acts as a threshold for the flow to be initiated, it is thought that in the case of low and mild yield stress, flow is easily initiated and the characteristic of flow phases are similar to viscous Newtonian fluid where inertial flow phase is dominant in low viscosity case and viscous flow phase is dominant in higher viscosity case[1)].

It is thought that in high yield stress cases, the flow could not be initiated immediately and a part of the inertia of the flow is used to overcome the yield

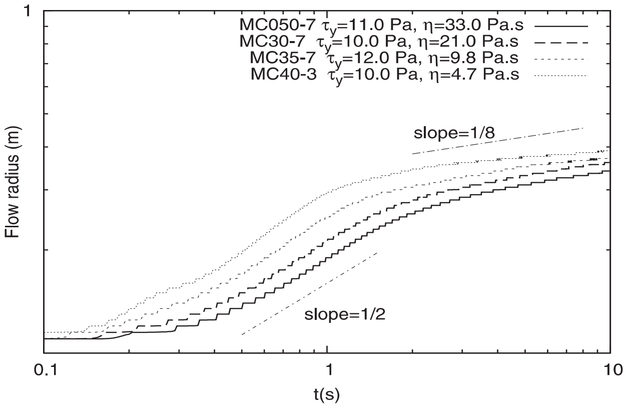

Fig. 6a Characteristic regions shown for front propagation of slump flow for relatively low yield stress cases.

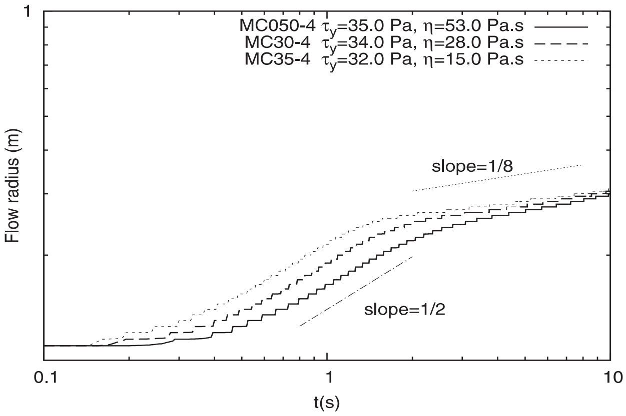

Fig. 6b Characteristic regions shown for front propagation of slump flow for relatively mild yield stress cases.

stress before the flow is initiated. Therefore the inertial flow phase is not distinct and the slope is less than $1/2$ in the initial range and thereafter followed by a distinct viscous flow phase. In the case of low yield stress, the slope is approaching to zero with the increase of time. It is thought that this represents the slowing down of the flow due to yield stress and the flow will finally reach a static state of pressure-yield stress balance.

8. CONCLUSION

In this study, a numerical model was developed to simulate the phenomena of slump flow test of fresh concrete. The numerical model performance was verified by comparing the numerical simulation results with the available experimental works. It was shown that the model could simulate the slump flow satisfactorily especially in the case where the ratio of η/τ_y is less than 1.0. However, in some cases the performance of the model was weaker. The author hopes to improve the numerical model performance by reconsidering the constitutive relations of Bingham fluid used in this study. The model was later used to verify the characteristic flow phases in Bingham fluid. It was shown that the model could reproduce the characteristic flow phases of Bingham fluid.

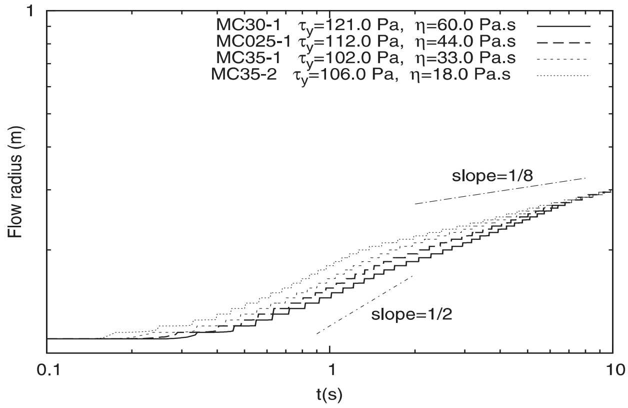

Fig. 6c Characteristic regions shown for front propagation of slump flow for relatively high yield stress cases.

REFERENCES

1) Puay, H. T. Hosoda, T.: Study of characteristics of inertial and viscous flow regions by means of dam break flow with finite volume, *J. App. Mech. JSCE,* Vol. 10,pp.757-768, 2007.
2) Huppert, H. E.: The propagation of two-dimensional and axisymmetric viscous gravity currents over a rigid horizontal surface, *J. Fluid. Mech.,* Vol. 121, pp.43-58, 1982.
3) Kokado, T., Hosoda, T., Miyagawa, T. and Fuji, M.: Study on a method of obtaining yield values of fresh concrete from slump flow test, *Concrete Lib. of JSCE*, Vol.32, pp.29-41, 1998.
4) Kokado, T., Hosoda, T. and Miyagawa, T.: Method for evaluating rheological coefficients of self-compacting concrete by numerical analysis, *Concrete Lib. of JSCE*, Vol.38, pp.51-69, 2001.
5) Hirt, C. W. and Nicholas, B. D.: Volume of fluid (VOF) method for the dynamics of free boundaries, *J. Comput. Phys.,* Vol.39, pp.201-225, 1981.
6) Fung, Y. C.: *A first course in continuum mechanics,* Prentice Hall, 1994.
7) Yabe, T., Ishikawa, T. and Wang, P. Y.: A universal solver for hyperbolic equations by cubic-polynomial interpolation II. Two- and three-dimensional solver, *Comput. Phys. Commun.*, Vol.66, pp.233-242, 1991.
8) Yamada, F., Takikawa, K., Iio, M.: Computational accuracy of the VOF method using the CIP method for solving advection of density functions, *J. App. Mech. JSCE*, Vol. 1, pp. 283-292, 1998.
9) Hosoda, T., Kokado, T. and Miyagawa, T.: Flow characteristics of viscous fluids on the basis of self-similarity law and its applications to high flow concrete, *J. App. Mech. JSCE*, Vol.3, pp.313-321, 2000.

(Received September 30, 2009)